JOURNAL OF GEOPHYSICAL RESEARCH, VOL. 106, NO. D7, PAGES 7281–7290, APRIL 16, 2001

Quasi-biennial oscillation in vertical velocity inferred from trace gas data in the equatorial lower stratosphere

Masanori Niwano and Masato Shiotani

Graduate School of Environmental Earth Science, Hokkaido University, Sapporo, Japan

Abstract. Vertical velocity variations associated with the quasi-biennial oscillation (QBO) in the equatorial lower stratosphere are investigated with the Halogen Occultation Experiment (HALOE) data from 1993 to 1998. The vertical velocity is inferred from ascent rates of an annual cycle in total water ($[H_2O] + 2[CH_4]$) profiles around the 20–60 hPa layer over the equator. The zonally averaged ascent rates of total water anomalies exhibit QBO-related variations with anomalies of 0.10–0.15 mm s^{-1} between 20 and 40 hPa at the equator, whereas there scarcely exists an annual cycle in the ascent rates. The QBO variation of the ascent rates shows that its positive anomalies precede negative anomalies of temperature and ozone variations by about 2–3 months at the equator and 30–60 hPa. This phase relationship is in conflict with former results from several two-dimensional model studies, which have reported that vertical velocity variations are almost out of phase with temperature anomalies preceding ozone anomalies by a few months. It is supposed that these differences could be caused by the observed large tendency of temperature anomalies, which is related to the observed rapid acceleration of the QBO westerly. An estimate of vertical advection of zonal momentum expected from the ascent rates suggests that the asymmetric acceleration of the zonal wind QBO can be explained by the QBO-induced vertical velocity being asymmetric between the easterly and the westerly shear zones.

1. Introduction

The meridional circulation induced by the quasi-biennial oscillation (QBO) was first indicated by *Reed* [1964] right after the discovery of the QBO signals in zonal wind, temperature [*Reed et al.*, 1961; *Veryard and Ebdon*, 1961], and ozone [*Funk and Garnham*, 1962; *Ramanathan*, 1963]. Reed inferred the vertical velocity variation with an amplitude of about 1×10^{-4} m s^{-1} over the equator and the phase reversal around 15° latitude. The idea of a two-cell structure being symmetric about the equator is supported by two-dimensional models [*Plumb and Bell*, 1982; *Dunkerton*, 1985]. Recent studies have emphasized that during the solstitial seasons the winter cell is strengthened, whereas the summer cell almost disappears [*Jones et al.*, 1998; *Kinnersley*, 1999; *Randel et al.*, 1999], in accordance with the observed ozone anomalies that are amplified at midlatitudes during winter-spring in each hemisphere [e.g., *Angell and Korshover*, 1978; *Hasebe*, 1983; *Randel and Wu*, 1996].

The vertical velocity oscillation has mainly three important roles in the whole QBO system. (1) The QBO-induced vertical velocity maintains the thermal wind balance in the face of radiative damping, so ascent anomalies are seen in the area of cold temperature anomalies, and vice versa [*Plumb and Bell*, 1982]. (2) The QBO-driven circulation transports ozone and other trace gases to produce their QBO signals mainly through the vertical transport [*Reed*, 1964; *Hasebe*, 1984]. Observational studies have reported the QBO variation in ozone [*Oltmans and London*, 1982; *Randel and Wu*, 1996] and in other constituents [*Zawodny and McCormick*, 1991; *Randel et al.*, 1998]. (3) The induced vertical velocity contributes to acceleration of the zonal wind QBO due to vertical advection of angular momentum. In westerly shear (warm) regions, descent anomalies lead to westerly acceleration, while in easterly shear (cold) regions, ascent anomalies induce easterly acceleration [*Plumb and Bell*, 1982; *Dunkerton*, 1991]. This could lead to the observed asymmetry in descent rates of the QBO shear regions [*Naujokat*, 1986].

In addition to these known roles of the QBO-induced meridional circulation, the variation can be the key to resolve the following two subjects recently under debate. One is the observed phase relationship between QBO signals in temperature and ozone in the tropics. Observational studies showed that the two variations are in phase in the lower stratosphere [*Randel and Cobb*, 1994]. *Hasebe* [1994] proposed that this in-phase relationship between the two oscillations is determined by the ozone-induced solar heating, which shifts the phase of the ozone QBO up to a quarter cycle earlier. The importance of the diabatic effects of the ozone QBO on the temperature QBO is emphasized by *Li et al.* [1995]. However, *Huang* [1996] pointed out that the ozone-induced solar heating variations are negligible in her two-dimensional model, including a radiative calculation. On the other hand, *Jones et al.* [1999] suggested that the QBO-induced horizontal velocity can generate rather large meridional advection of ozone to produce the observed phase relationship between ozone and temperature. In spite of these efforts, the phase relationship between the QBO signals of vertical velocity, temperature, and ozone is still ambiguous in each study [e.g., *Ling and London*, 1986; *Jones et al.*, 1999; *Randel et al.*, 1999].

The other problem is the momentum source required to produce the observed zonal wind QBO, which shows more

Paper number 2000JD900798.
0148-0227/01/2000JD900798$09.00

rapid acceleration of westerlies than easterlies [*Dunkerton and Delisi*, 1985; *Naujokat*, 1986]. The zonal wind oscillation has been explained by momentum deposit of vertically propagating waves from the tropical troposphere, as proposed by *Lindzen and Holton* [1968] and *Holton and Lindzen* [1972]. In addition, the QBO acceleration can also be affected by the QBO-driven and the time mean vertical velocity [*Plumb and Bell*, 1982; *Gray and Pyle*, 1989; *Dunkerton*, 1991; *Dunkerton*, 1997]. The observed phase asymmetry of zonal wind acceleration can be generated by the asymmetry of wave momentum flux [*Holton and Lindzen*, 1972; *Takahashi et al.*, 1997], as well as by that of vertical advection [*Plumb and Bell*, 1982; *Kinnersley and Pawson*, 1996]. The former effect is inferred from observational studies of equatorial Kelvin and gravity waves with periods longer than 1 day in rawinsonde data [*Maruyama*, 1994; *Sato et al.*, 1994; *Sato and Dunkerton*, 1997] and satellite data [*Wu and Waters*, 1996; *Canziani and Holton*, 1998]. However, the behavior of the equatorial waves with periods shorter than 1 day and Rossby waves from middle latitudes should be examined quantitatively.

To solve the two problems mentioned above, observations of the QBO-induced vertical velocity are indispensable. However, direct measurements of the mean meridional circulation in the stratosphere are not yet available, since the magnitude of the circulation is very small. The meridional circulation has been estimated mainly with the two ways; one is based on the diabatic heating rates [*Murgatroyd and Singleton*, 1961; *Dunkerton*, 1978; *Rosenlof*, 1995] and the other is from the momentum and heat flux divergence [*Haynes et al.*, 1991; *Holton*, 1990; *Rosenlof and Holton*, 1993]. Recently, ascent signals of water vapor anomalies have been observed from the Upper Atmosphere Research Satellite (UARS) [*Mote et al.*, 1995, 1996; *Jackson et al.*, 1998; *Randel et al.*, 1998]. *Mote et al.* [1998] (hereinafter referred to as M98) investigated mean ascent rates of annually varying signals of total water (water vapor plus twice methane) in the tropical lower stratosphere by using trace gas data from the Halogen Occultation Experiment (HALOE) aboard UARS and derived the Lagrangian mean vertical velocity from the ascent rates.

The purpose of this paper is to clarify observational features of the QBO-related variations in the ascent rate of total water anomalies in the tropical lower stratosphere by using the HALOE trace gas data. It is noted that our analysis of the ascent rate is extended to its time variations, while the analysis by *Mote et al.* [1998] was limited to time mean field averaged within 15° of the equator. Furthermore, we also calculate four kinds of ascent rates and discuss differences between the four. We emphasize that *Randel et al.* [1998] examined the QBO signals seen in water vapor profiles but that we investigate the QBO variations in the ascent rates.

The data used for our analysis and the calculation of ascent rates of water vapor anomalies are presented in section 2. The QBO components of the derived ascent rate are shown in section 3. The QBO-induced variations are described especially in terms of the amplitude and phase at the equator, with the help of Singapore temperature and zonal winds, and HALOE ozone data. Furthermore, we examine the vertical advection effect of zonal momentum, using the derived ascent rates of total water anomalies. Finally, a summary is given in section 4.

2. Data

2.1. HALOE Trace Gas Data

In this study we will use water vapor, methane, and ozone profiles from the HALOE version 18 data for the period of January 1993 to April 1998. The HALOE instrument is described by *Russell et al.* [1993]. The instantaneous vertical field of view is 1.6 km at the Earth limb. The HALOE data (level 2) are available on pressure levels of $1000 \times 10^{-(i/30)}$ hPa (i = 0, 1, ...), corresponding to a vertical spacing of about 0.5 km. HALOE is a solar occultation instrument which performs 15 observations at both sunrise and sunset everyday. The observation points for each sunrise and sunset are located on about one latitudinal circle at about 25° longitude intervals, though shifting latitudinally with time. In the tropics, measurements are made about 10 times per year [*Russell et al.*, 1993, Figure 8].

For our analysis, a zonal mean profile is constructed by averaging 15 sequential observations, the center of which is closest to each latitudinal grid with a 2.5° interval. The obtained values correspond to the average of profiles over about 5° around the equatorial latitudes. We only use the zonal mean data because the QBO variation generally shows zonally uniform phase change in the tropical lower stratosphere [*Shiotani*, 1992; *Shiotani and Hasebe*, 1994].

To derive an ascent rate of annually varying signals of water vapor, we use total water ($\hat{H} = [H_2O] + 2[CH_4]$). Total water is approximately conserved in the middle atmosphere, because the chemical dissociation of a methane molecule provides two water molecules [*Jones et al.*, 1986; *Dessler et al.*, 1994; *Remsberg et al.*, 1996]. The HALOE water vapor and methane profiles (version 18) show differences between sunrise and sunset in the lower stratosphere with sunset data being larger than sunrise data. This problem of accuracy suggests that we had better calculate the ascent rate of the $\hat{H}$ anomaly rather than $\hat{H}$ directly. The zonal mean data of water vapor and methane are spline-interpolated in time, when the missing period is within 4 months; otherwise no interpolation is carried out with respect to time. After the time average is removed, the temporal variations of water vapor and twice methane are added up. We note again that these data keep information on the original observation time.

The ascent rate w_{tr} of total water anomalies (which is called a tape recorder signal by *Mote et al.* [1996]) is derived from time-pressure profiles at each latitude, by following a phase line of $\hat{H}$ anomalies. Here we consider four phases, $\chi = 0$, $\chi_t = 0$, $\chi_z = 0$, and $\chi_{zt} = 0$, where χ is the annually varying component of $\hat{H}$ volume mixing ratio, and the subscripts t and z indicate differentiation with respect to time and log-pressure height, respectively. By following the four phases we can get four kinds of w_{tr} ($w_{tr}|_{\chi=0}$, $w_{tr}|_{\chi_t=0}$, $w_{tr}|_{\chi_z=0}$, and $w_{tr}|_{\chi_{zt}=0}$ for $\chi = 0$, $\chi_t = 0$, $\chi_z = 0$, and $\chi_{zt} = 0$, respectively). In a case of $\chi_z = 0$, we first find out a vertical grid point $z|_{\chi_z=0}$ nearest to $\chi_z = 0$ at all time steps (Figure 1). Then, we differentiate two values at adjacent points $z(t_1)$ and $z(t_2)$ on each $\chi_z = 0$ line at adjacent time steps t_1 and t_2 in order to obtain $w_{tr}|_{\chi_z=0}$; that is, $w_{tr}|_{\chi_z=0} = [z(t_2) - z(t_1)]_{\chi_z=0}/(t_2 - t_1)$. In a similar way, we can obtain w_{tr} for the other phase lines. Note that the results shown in M98 are based on only $w_{tr}|_{\chi=0}$ and $w_{tr}|_{\chi_t=0}$. The derived w_{tr} is assumed to be located in the middle of the original two points with respect to time and altitude. It is emphasized that $\hat{H}$ data keep their observed time. We per-

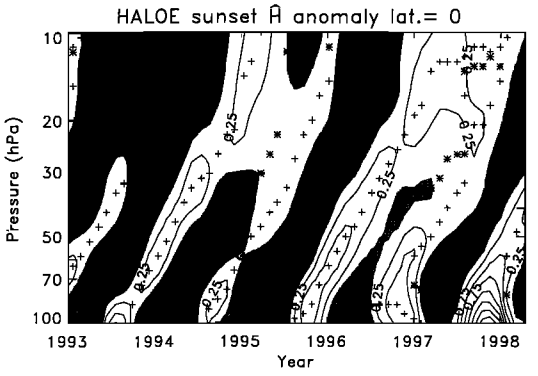

Figure 1. Time-height section of $\hat{H}$ anomalies at the equator from HALOE sunset data. $\hat{H}$ anomalies are defined as departures from the time mean of $\hat{H}$ after 1992. Contour interval is 0.25 ppmv, with negative values stippled. Vertical maxima and minima are indicated by pluses and asterisks, respectively.

formed these calculations for sunrise and sunset data separately, since sunrise data of water vapor have a small bias in the lower stratosphere.

Here we briefly examine features of the ascent motion of total water anomalies in the meridional plain with respect to the amplitude and phase of annual components of $\hat{H}$ (Figure 2). Figure 2a presents the equivalent harmonic amplitude, calculated as a RMS value times $\sqrt{2}$ [*Randel et al.*, 1999]. It shows that the annual amplitude of $\hat{H}$ anomalies decreases with height. The decay rate is small between about 20 and 50 hPa

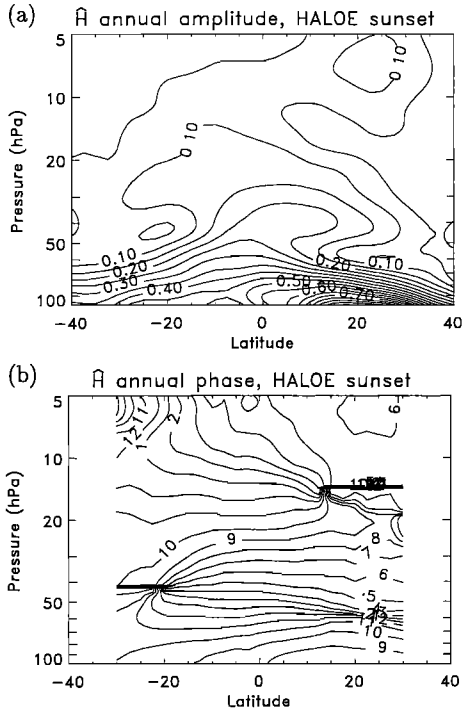

Figure 2. Latitude-height cross sections of the equivalent harmonic amplitude (a) and the phase (b) of annual components of $\hat{H}$ from HALOE sunset data. The annual components of $\hat{H}$ are reconstructed by annual and semiannual components of climatological monthly data based on $\hat{H}$ data from 1993 to 1998. Contour intervals are 0.05 ppmv (a) and months with maximum annual anomalies (b).

within 15° of the equator. We note that at low latitudes below 60 hPa, amplitudes are larger in the Northern Hemisphere than in the Southern Hemisphere [*Rosenlof*, 1997]. The phase of the annual component of $\hat{H}$ is presented in Figure 2b. It is clear to see a phase rising with time between 15°N and 15°S, which is latitudinally constant in the 15–60 hPa layer. These figures suggest that the ascent of the annual component of $\hat{H}$ is mainly determined by vertical advection, consistent with results in M98.

In this paper the QBO components of ascent rate and ozone are defined as deviations from the climatological seasonal cycle. The climatological monthly mean data are constructed with use of data during the period of January 1993 to April 1998, since water vapor data are not available in the equatorial lower stratosphere in 1991 and 1992 under the condition of elevated aerosol due to the Mount Pinatubo eruption. Using Fourier annual and semiannual components plus time mean, we reconstruct the climatological annual cycle. After the reconstructed annual cycle is subtracted from the original time series of zonal mean ascent rate and ozone, we smooth the deseasonalized data by removing components with periods shorter than 3 months. Finally, the sunrise and sunset data are mixed in time order. Note that these data are not binned into monthly samples but keep the original observation time information.

2.2. Singapore Rawinsonde Data

To study a relation to the QBO-induced variations in vertical velocity, we use temperature and zonal wind data at Singapore (1.4° N, 104.0° E) from January 1991 to December 1997. Singapore data are generally used as a reference of a zonal mean value, since in the equatorial regions there exist rawinsonde observations for a long time period only at Singapore. The use of Singapore temperature data in place of zonal mean values at the equator is supported by near agreement between the temperature QBO at Singapore and the zonal mean temperature QBO in the U.K. Meteorological Office (UKMO) data with respect to the phase [*Randel et al.*, 1999]. Observations of the ozone QBO also show zonally uniform phase changes [*Shiotani*, 1992; *Shiotani and Hasebe*, 1994].

The twice daily data at standard and significant levels are interpolated to the same pressure levels as HALOE data with use of the Hermite polynomials. Then, the daily data are produced by averaging two profiles a day. The calculation of QBO components in temperature and zonal wind follows the same way as in the HALOE ozone but for a climatological annual cycle based on the daily data.

3. Comparisons Among Four Kinds of w_{tr}

In this section we will show the four kinds of derived w_{tr} in terms of the temporal variation and time mean component and investigate differences between the four.

3.1. Time Variations

Temporal variations of the four kinds of w_{tr} at 40 hPa are shown in Figure 3. The most remarkable feature is that QBO-related variations are prominent in almost all kinds of w_{tr} without excluding the annual cycles. We note that the three estimates $w_{tr}|_{\chi=0}$, $w_{tr}|_{\chi_z=0}$, and $w_{tr}|_{\chi_{tz}=0}$ show clear QBO variations at this level. On the other hand, $w_{tr}|_{\chi_t=0}$ generally shows unclear QBO signals relative to the other three w_{tr} at most of the altitudes. This may be because the HALOE data

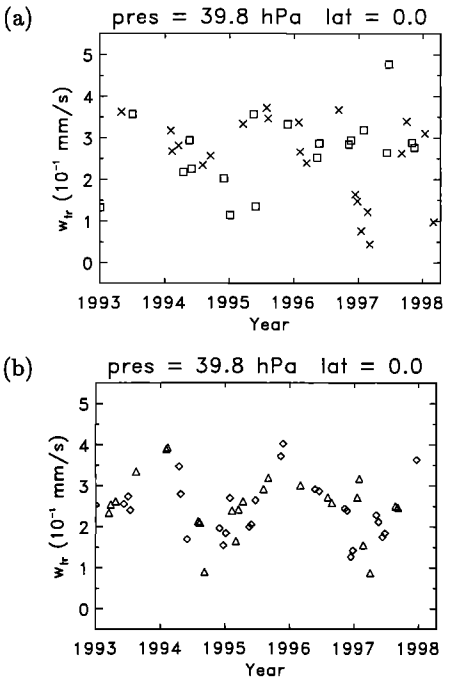

Figure 3. Time sequences of four kinds of w_{tr} at the equator at 40 hPa. (a) $w_{tr}|_{\chi=0}$ (crosses) and $w_{tr}|_{\chi_t=0}$ (squares), and (b) $w_{tr}|_{\chi_z=0}$ (diamonds) and $w_{tr}|_{\chi_{tz}=0}$ (triangles). The data within ±600 m of the altitude are also plotted.

retrieval has a better vertical resolution than a time resolution, resulting in poor accuracy of χ_t. Furthermore, data sampling of $w_{tr}|_{\chi=0}$ is extremely coarse above 30 hPa because $\chi = 0$ contours get closed there in late 1993 and early 1995 and 1997 (Figure 1). For the analysis of the QBO variation, therefore, we had better use $w_{tr}|_{\chi_z=0}$ and $w_{tr}|_{\chi_{tz}=0}$ rather than the other two used in M98. It is also emphasized that the annual cycle cannot be clearly seen in Figure 3, conflicting with brief estimates of *Mote et al.* [1996].

3.2. One-Dimensional Model of Trace Constituents by M98

To discuss the difference between the four kinds of w_{tr} and the Lagrangian vertical velocity in terms of time mean and QBO variations, we follow a one-dimensional model of trace constituents used in M98. The zonal mean of trace constituent distribution is supposed to be simply expressed by advection, diffusion, dilution, and sink/source terms as

$$\chi_t + w\chi_z = \frac{1}{\rho_0}(\rho_0 K\chi_z)_z - \alpha(\chi - \chi_{\mathrm{ML}}) + S, \tag{1}$$

where χ represents a trace constituent volume mixing ratio, w is the Lagrangian vertical velocity, ρ_0 is a basic density given by $\rho_0 = \rho_s e^{-z/H}$ with the scale height $H = 7$ km and the log-pressure height $z = -H \ln (p/p_s)$, where the subscript s means a constant reference value, $\chi_{\mathrm{ML}} = \chi_{\mathrm{ML}}(z)$ means a tracer mixing ratio around the midlatitudes, K denotes a vertical diffusion coefficient, α indicates a relaxation rate to a midlatitude value χ_{ML}, and S is the chemical sink and source term. Equation (1) can be rewritten as

$$\chi_t + \bar{w}\chi_z = K\chi_{zz} - \alpha(\chi - \chi_{\mathrm{ML}}) + S, \tag{2}$$

where

$$\bar{w} \equiv w + K/H - K_z. \tag{3}$$

Here we may suppose χ to be $\hat{H}$ anomalies. Since $\hat{H}$ is approximately preserved with a nearly constant value of 6.8 ppmv in the middle atmosphere [*Randel et al.*, 1998], it is supposed that the midlatitude value of $\hat{H}$ is spatially and temporally constant at the mean value of $\hat{H}$ in the tropics. Then, we have $S = 0$ and $\chi_{\mathrm{ML}} = 0$, and we can rewrite (2) as

$$\chi_t + \bar{w}\chi_z = K\chi_{zz} - \alpha\chi. \tag{4}$$

When ascent rates of $\chi = 0$ (denoted by $w_{tr}|_{\chi=0}$ hereinafter) are considered, χ still remains zero at the reference frame moving with $\chi = 0$ lines at $w_{tr}|_{\chi=0}$. Therefore we have an expression as

$$\chi_t + w_{tr}|_{\chi=0}\chi_z = 0. \tag{5}$$

By using (4) and (5), we obtain the relationship between w and $w_{tr}|_{\chi=0}$

$$w_{tr}|_{\chi=0} = w + \frac{K}{H} - K\left.\frac{\chi_{zz}}{\chi_z}\right|_{\chi=0} - K_z. \tag{6}$$

In the same way as in M98 we can examine the relationship between w and ascent rates of $\chi_t = 0$, $\chi_z = 0$, and $\chi_{tz} = 0$ (not shown). For time mean and QBO components these relationships are shown in the following subsections.

3.3. Time Mean Components

The time mean of four kinds of w_{tr} is given in Figure 4. This shows that all four range between 0.2 and 0.35 mm/s and are larger in the 20–40 hPa layer than in the 40–70 hPa layer. In spite of the similarities, we notice that $w_{tr}|_{\chi=0}$ and $w_{tr}|_{\chi_t=0}$ are clearly distinguished from $w_{tr}|_{\chi_z=0}$ and $w_{tr}|_{\chi_{tz}=0}$. There is a clear vertical minimum of 0.22–0.24 mm/s near 50 hPa only in $w_{tr}|_{\chi=0}$ and $w_{tr}|_{\chi_t=0}$, which are examined in M98. On the contrary, $w_{tr}|_{\chi_z=0}$ and $w_{tr}|_{\chi_{tz}=0}$ show nearly constant values of 0.25–0.275 mm/s over 35–60 hPa.

We try to understand these differences using the one-dimensional formulation for the time mean field as below:

$$w_{tr}|_{\chi=0} = w + \frac{K}{H} - K\left.\frac{\chi_{zz}}{\chi_z}\right|_{\chi=0} - K_z, \tag{7}$$

$$w_{tr}|_{\chi_t=0} = w + \frac{K}{H} - K\left.\frac{\chi_{tzz}}{\chi_{tz}}\right|_{\chi_t=0} - K_z, \tag{8}$$

$$w_{tr}|_{\chi_z=0} = w + \frac{K}{H} - 2K_z - \left(K\frac{\chi_{zzz}}{\chi_{zz}} - \alpha_z\frac{\chi}{\chi_{zz}}\right)_{\chi_z=0}, \tag{9}$$

$$w_{tr}|_{\chi_{tz}=0} = w + \frac{K}{H} - 2K_z - \left(K\frac{\chi_{tzzz}}{\chi_{tzz}} - \alpha_z\frac{\chi_t}{\chi_{tzz}}\right)_{\chi_{tz}=0}. \tag{10}$$

It is notable that $w_{tr}|_{\chi=0}$ is almost the same form as $w_{tr}|_{\chi_t=0}$, but χ_z is included instead of χ_{tz}. In a similar way, $w_{tr}|_{\chi_z=0}$ and $w_{tr}|_{\chi_{tz}=0}$ are almost the same except that the former includes χ in place of χ_t.

M98 has shown that time mean w_{tr} (from $w_{tr}|_{\chi=0}$ and $w_{tr}|_{\chi_t=0}$) is quite close to the Lagrangian vertical velocity w, and the difference between w and w_{tr} is less than 0.03 mm/s between 30 and 70 hPa. The observed difference between w_{tr} of $\chi = 0$ and $\chi_t = 0$, and w_{tr} of $\chi_z = 0$ and $\chi_{tz} = 0$ (Figure 4a), can be explained by $-K_z$ and α-related term, which are the differences between (7) and (8), and (9) and (10). For time

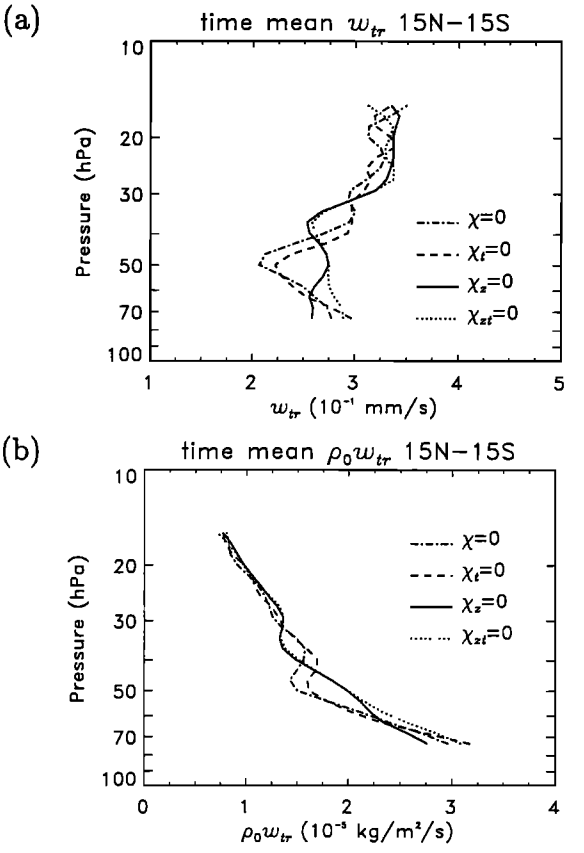

Figure 4. Mean vertical profiles of four kinds of w_{tr} (a) and that multiplied by density (b) $w_{tr}|_{\chi=0}$ (dashed-dotted line), $w_{tr}|_{\chi_t=0}$ (dashed line), $w_{tr}|_{\chi_z=0}$ (solid line), and $w_{tr}|_{\chi_{tz}=0}$ (dotted line), which are averaged within ±15° latitude of the equator. The calculation of mean values is based on data from 1993 to 1998.

mean we use the mixture of $w_{tr}|_{\chi=0}$ and $w_{tr}|_{\chi_t=0}$ as a proxy for the Lagrangian mean vertical velocity in this study.

Here we also focus on a brief estimate of horizontal flow which leaks out of tropical upward mass flow. Figure 4b shows mean vertical velocity weighted by a density factor. We notice that a decrease of $w_{tr}|_{\chi=0}$ and $w_{tr}|_{\chi_t=0}$ with increasing height slows down in the 35–50 hPa layer. Because of near conservation of vertical mass flux, it is expected that the air is mostly advected upward with little latitudinal attenuation in this altitude range where there exist strong mixing barriers at the subtropics, corresponding to Figure 2. Since the poleward flow in the equatorial regions may be driven by damping of Rossby waves at low latitudes [*Plumb and Eluszkiewicz*, 1999], near conservation of vertical mass flux implies that there exists little tropical intrusion of Rossby waves from midlatitudes in this layer. Above 35 hPa the vertical mass flow decreases more rapidly. The mass flux becomes half from 35 to 15 hPa (~5 km), with a constant decreasing rate in this layer. Below 60 hPa a decrease rate of vertical mass flow is about the largest in Figure 4b and reaches 1.5×10^{-5} kg/m²/s per 3 km (55–75 hPa).

3.4. QBO Variations

We briefly discuss the difference between w and the four kinds of w_{tr} with respect to the QBO components. Neglecting the annual component (Figure 3), we obtain the relationship between w, and $w_{tr}|_{\chi=0}$ and $w_{tr}|_{\chi_z=0}$ for the QBO components (denoted by a subscript B) as follows:

$$w_{trB}|_{\chi=0} = w_B, \tag{11}$$

$$w_{trB}|_{\chi_z=0} = w_B + \alpha_{Bz} \left.\frac{\chi}{\chi_{zz}}\right|_{\chi_z=0} \tag{12}$$

under the assumption $K(t, z) \approx K(z)$.

It is expected from (11) that $w_{trB}|_{\chi=0}$ is a first approximation to the actual Lagrangian mean vertical velocity w_B. Our results show that $w_{trB}|_{\chi_z=0}$ is nearly close to $w_{Btr}|_{\chi=0}$ around 40 hPa but that it is 0.03 mm/s smaller than $w_{Btr}|_{\chi=0}$ at 30 hPa. The difference between w_B and $w_{trB}|_{\chi_z=0}$ can be quantified by the second term $\alpha_{Bz}\chi/\chi_{zz}|_{\chi_z=0}$ on the right-hand side of (12). In the following section, the QBO component of $w_{tr}|_{\chi_z=0}$ will be shown instead of w_B, as mentioned in section 3.1. To increase the number of data, we also use $w_{tr}|_{\chi_{tz}=0}$, showing almost the same QBO variations as $w_{tr}|_{\chi_z=0}$ (Figure 3b). It should be kept in mind that the real w may exhibit larger anomalies than the mixture of $w_{tr}|_{\chi_{tz}=0}$ and $w_{tr}|_{\chi_z=0}$ around 30 hPa.

4. Results

4.1. Observational Results

Here we clarify the observed feature of the QBO variation of w_{tr} based on $w_{tr}|_{\chi_z=0}$ and $w_{tr}|_{\chi_{tz}=0}$ at the equator. Figure 5 clearly shows the QBO variations in w_{tr}. The equatorial upwelling ranges between 0.1 and 0.5 mm/s around the time mean of 0.25–0.30 mm/s in the 20–40 hPa layer. The anomalies of the QBO signal reaches 0.10–0.15 mm/s between 20 and 40 hPa and is less than 0.1 mm/s at the 50-hPa level. It is also clear that the variation is roughly out of phase with temperature anomalies at all altitudes, as expected from a balance between the Newtonian cooling and the adiabatic vertical motions.

We also note almost no difference between the deseasonalized component and the raw data in Figure 3. This indicates that there exists only a little annual cycle of mean upwelling in this layer. The observed annual cycle in this study has an amplitude of around 0.03–0.04 mm/s in the 30–50 hPa layer and more than 0.05 mm/s at 20 and 50–70 hPa. The observed annual cycles in ascent rates are about half of QBO variations between 30 and 40 hPa and are comparable with those at 20 and 50–70 hPa. In the lowermost stratosphere a strong annual cycle of residual vertical velocity has been reported by several studies [cf. *Rosenlof*, 1995], computing residual circulation from radiative calculation. However, our results emphasize that in the 30–40 hPa layer the QBO variations could be dominant in vertical velocity.

The derived QBO variation of ascent rates of total water anomalies appears to be larger than results deduced from heating calculations. Furthermore, it is possible that the actual vertical velocity could have larger QBO components than w_{tr} (of $\chi_z = 0$ and $\chi_{tz} = 0$), as mentioned in section 3.4. *Randel et al.* [1999] presented the residual mean vertical velocity $\overline{w^*}$ by computing heating rates calculated from a radiation code of *Olaguer et al.* [1992] and HALOE trace gas data and UKMO temperature anomalies increased by a factor 1.4 as input. The maximum QBO anomaly is 0.24 km/month (~0.10 mm/s) at 32 hPa [*Randel et al.*, 1999], which is about two thirds of our results (~0.15 mm/s). This disagreement may be related to a

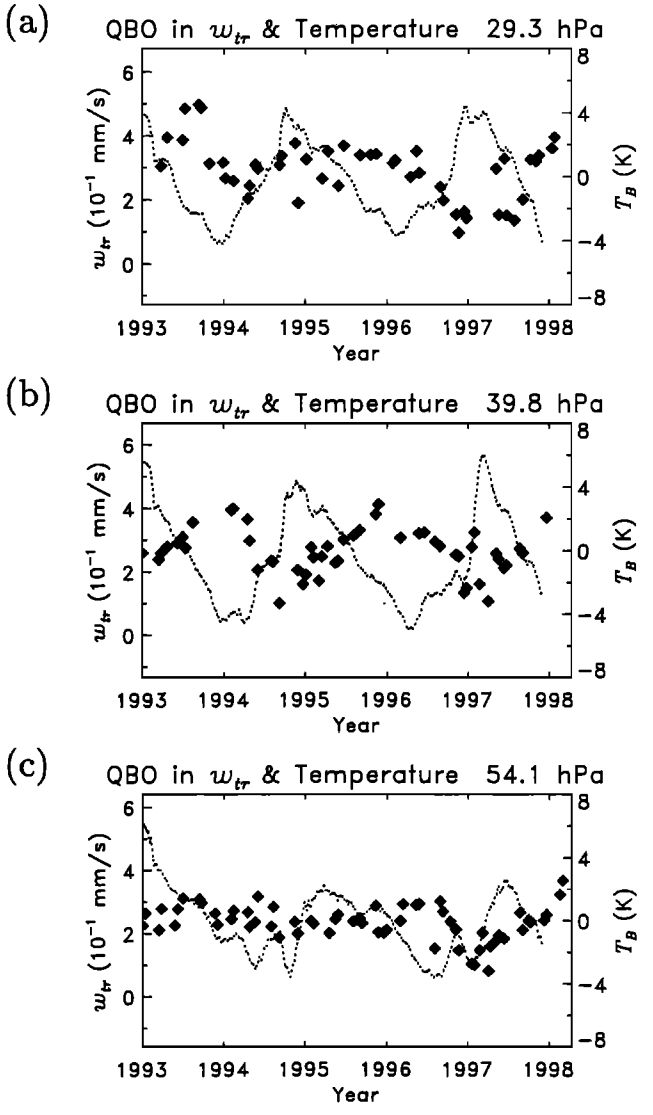

Figure 5. Same as in Figure 3 but for deseasonalized components of w_{tr} (based on $w_{tr}|_{\chi_z=0}$ and $w_{tr}|_{\chi_{tz}=0}$) plus time mean (from $w_{tr}|_{\chi=0}$ and $w_{tr}|_{\chi_t=0}$) at 30 hPa (a), 40 hPa (b), and 54 hPa (c). The QBO components in Singapore temperature (dotted lines) are also plotted for reference.

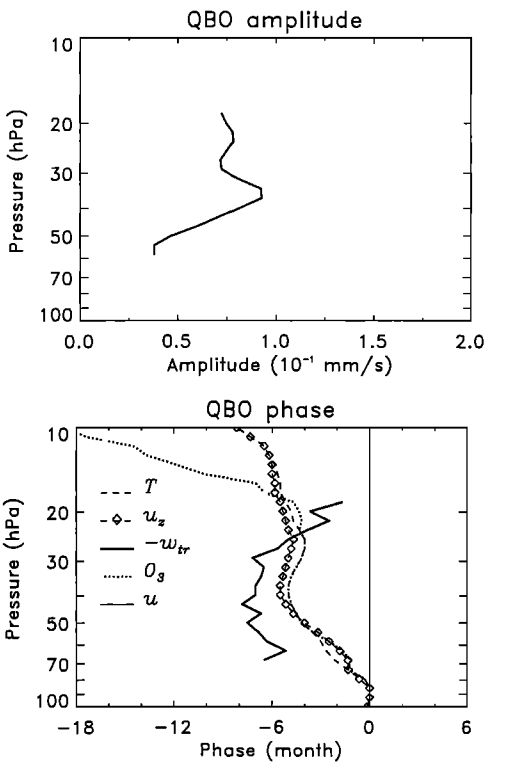

Figure 6. Vertical profiles of (a) the QBO amplitude of w_{tr} and (b) the QBO phases of subsidence anomalies in w_{tr} (thick solid line with horizontal lines), ozone (dotted line), zonal wind shear (dashed line with diamonds), and temperature (dashed line) relative to zonal wind oscillation (thin solid line) at the equator. Negative phases mean that the QBO signal in each quantity precedes zonal wind oscillation.

problem in the radiation scheme [*Olaguer et al.*, 1992], which is used to calculate the residual mean circulation.

Next, we examine the vertical distribution of the amplitude and phase of the QBO components at the equator. The amplitude and phase are derived by fitting the QBO variation in w_{tr} using a linear regression of the form

$$w_{trB}(t) = aT_B(t + b), \tag{13}$$

where T is Singapore temperature, the subscript B indicates the QBO component, $a(z)$ is a regression coefficient and $b(z)$ is the phase of w_{trB} compared to T_B. The amplitude is defined as the equivalent harmonic amplitude of the temperature QBO multiplied by the regression coefficient a. The phase is regarded as a lag such that a lag correlation between w_{trB} and T_B takes a maximum coefficient. The lag correlation is calculated by shifting w_{trB} relative to T_B by every 10 days. The amplitude and phase are plotted only if a maximum correlation coefficient is statistically significant at the level of 99.5%. The equivalent harmonic amplitude of the QBO signals in w_{tr} is shown in Figure 6a. There exists a large magnitude of the amplitude in the 20–40 hPa, roughly corresponding to the large magnitude of the temperature variation in this layer.

Figure 6b shows the phase of the QBO signals in w_{tr}, temperature, ozone, zonal wind, and its vertical shear. The phases of five quantities are derived from a calculation of lag correlations among temperature and other quantities and then shifted by setting the phase of the zonal wind QBO to zero. It is notable that temperature and ozone are just in phase below 20 hPa, and there is a lag of 2–3 months between $-w_{tr}$ and temperature and ozone in the 30–60 hPa layer. The phase lag between w_{tr} and temperature can also be seen in Figure 5.

Observational studies reported the in-phase relationship between temperature and ozone, using column ozone data [*Randel and Cobb*, 1994]. This result also coincides with that in the work of *Hasebe* [1994], who reproduced the ozone variation with use of Singapore zonal wind data. However, the observed phase relationship among vertical velocity, temperature, and ozone is in conflict with results from the conventional models considering only dynamics [*Reed*, 1964] and several two-dimensional models [e.g., *Jones et al.*, 1999]. In their models, negative anomalies of vertical velocity and temperature anomalies are almost in phase and the two precede ozone anomalies by several months (about a quarter cycle) in the lower stratosphere. Similarly, *Randel et al.* [1999] have also reported a high negative correlation when the lag is zero between the QBO

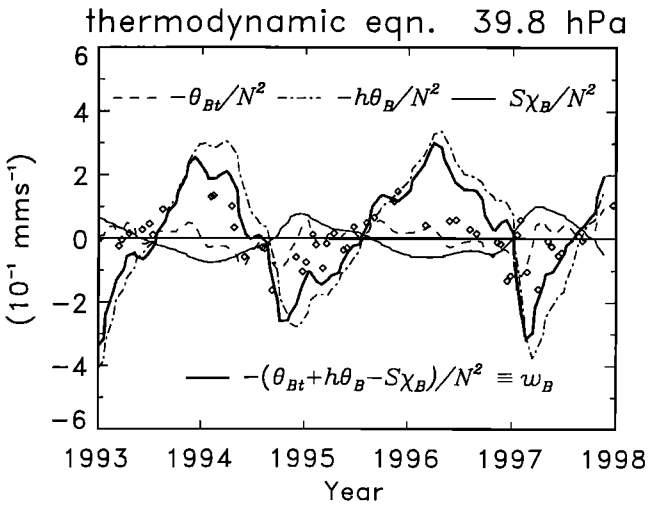

Figure 7. Time series of vertical wind velocity component estimated from equation (14); components from tendency term (dashed line), those from the Newtonian cooling term (dashed-dotted line), those from diabatic heating term owing to solar absorption by the ozone QBO (thin solid line) and those from the adiabatic heating term (thick solid line) calculated from the three terms above; w_{tr} (diamonds) is also plotted for reference.

signals of residual vertical velocity and vertical shear of the UKMO zonal winds in the lower stratosphere.

To examine the observed phase of the QBO signal in w_{tr}, we calculate vertical velocity indirectly from the thermodynamic equation, using the observed temperature and ozone data and compare them with the observed variation of w_{tr} in terms of the phase. We use a one-dimensional model of *Ling and London* [1986], which includes parameterized radiative effects, and a vertical advection term.

The thermodynamic equation is given as

$$\theta_{Bt} + w_B N^2 = -h\theta_B + S\chi_B, \tag{14}$$

following the notation of *Hasebe* [1994], where $\theta = RT/H$ is a buoyancy acceleration with the gas constant R for dry air, temperature T, and the scale height H, w is the Lagrangian mean vertical velocity, N is the buoyancy frequency, h is the Newtonian cooling coefficient, S represents the diabatic heating rate from solar absorption by ozone anomalies, χ denotes volume mixing ratio of ozone, the suffix B denotes the QBO component, and the subscripts t indicate a partial derivative with respect to time.

Figure 7 shows the calculated vertical velocity inferred from (14) and also the observed zonal mean ascent rates for reference. The inferred vertical velocity is divided into three parts: a component from the tendency term $(-\theta_{Bt}/N^2)$, that from the Newtonian cooling term $(-h\theta_B/N^2)$, and that of ozone solar heating $(S\chi_B/N^2)$. The inferred vertical velocity variation is determined by the dominant contribution from the Newtonian cooling term during the warm and cold periods (Figure 5). However, the variation is weakened by the contribution from the ozone QBO-induced solar heating [*Hasebe*, 1994; *Li et al.*, 1995], which is out of phase with the contribution from the Newtonian cooling. It should be emphasized that the component due to the ozone heating cannot affect the phase of vertical velocity, because the two terms on the right-hand side of (14) are out of phase (Figure 6).

On the other hand, a contribution from the temperature tendency precedes that from the Newtonian cooling by a quarter cycle. The negative anomalies are as large as about a third of the contribution from the Newtonian cooling term during the northern winter in 1994/1995 and 1996/1997. This large anomaly of the temperature tendency puts forward the phase of vertical velocity w_B relative to the component from the Newtonian cooling term by a few months. As a result, vertical velocity anomalies are precedent to negative anomalies of temperature and ozone by about 2 months. The inferred vertical velocity is nearly consistent with observations (w_{tr}) in terms of phase. Hence the temperature tendency can be important in determining the phases of vertical velocity and temperature. Some studies with models show the out-of-phase relationship between the two with little lag [*Huang*, 1996; *Jones et al.*, 1999]. Our results suggest that the models may underestimate the temperature tendency relative to the observations. To examine the phase relationship between QBO signals by using models, therefore, it may be necessary that models should represent the large temperature tendency associated with the rapid acceleration of the QBO wind.

4.2. Vertical Advection of Zonal Momentum Estimated From w_{tr}

Next, we examine the role of vertical advection of zonal momentum due to time mean and QBO-induced vertical velocity, by calculating each term in the zonal momentum equation at the equator from observed zonal winds and ascent rates of total water anomalies. We furthermore deduce wave momentum flux required to drive the observed zonal wind QBO.

We consider a simple zonal momentum equation expressed as

$$u_{Bt} = -(w_B + w_M)u_{Bz} + G \tag{15}$$

near the equator, where the subscript M denotes a time average component, and G includes the divergence of wave momentum flux, horizontal advection, and unresolved processes. In the following, we removed the annual component of w_{tr} to focus on the mean and QBO signals of w_{tr}. The time mean of w_{tr} is slightly larger than that of w by less than 0.05 mm/s, but the two are almost the same at 40 hPa (M98, Figure 9). However, the temperature QBO in Singapore may be exaggerated compared to zonal mean values, and then the following results may overestimate the magnitude of variations.

Figure 8a shows that zonal wind acceleration due to the vertical advection is about -1×10^{-6} m s^{-2} at this level for the westerly acceleration phase of the zonal wind QBO but that it reaches $+2 \times 10^{-6}$ m s^{-2} during the easterly acceleration phase. In Figure 8b the zonal wind tendency by vertical velocity anomalies $(-w_{trB}u_{Bz})$ calculated from the QBO component of w_{tr} always has positive anomalies of $\sim 1 \times 10^{-6}$ m s^{-2}; the QBO-induced vertical velocity helps the descent of the westerly shear, whereas delaying that of the easterly shear. This effect contributes to the observed asymmetry of zonal wind acceleration [*Plumb and Bell*, 1982].

Variations of G inferred from observed zonal wind and ascent rates of total water anomalies are also shown in Figure 8a. The most surprising feature is that deviations of G have almost the same maximum magnitudes of 5×10^{-6} m s^{-2} both during the easterly and the westerly acceleration phases of the zonal wind QBO at this altitude. We also see this feature of the G variation below 35 hPa. It is anticipated that the well-known

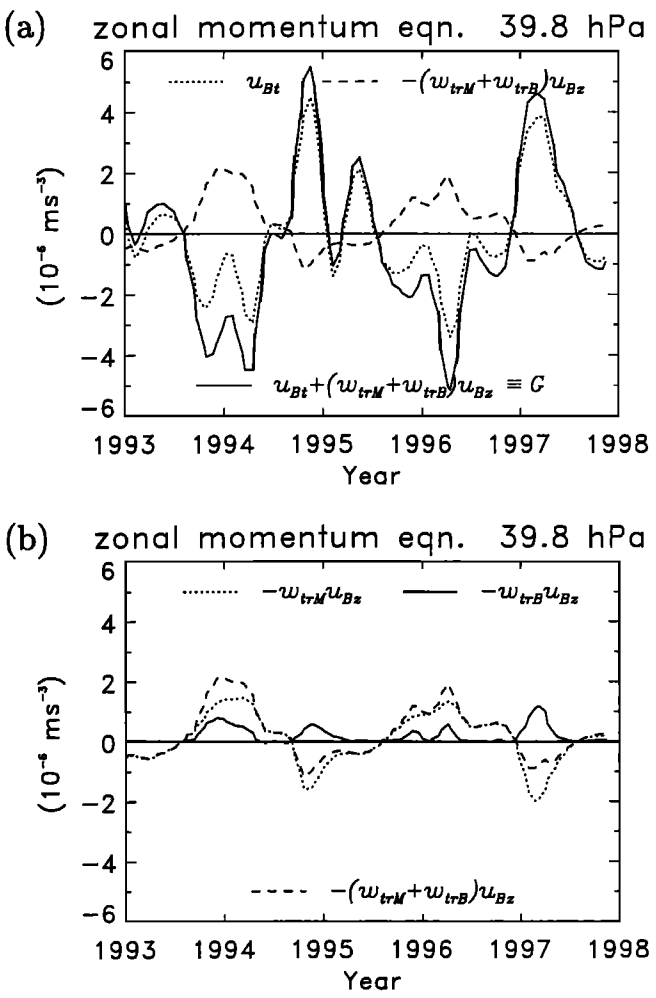

Figure 8. Time series of each term in the zonal momentum equation. (a) Tendency (dotted line) of the zonal wind QBO, vertical momentum advection (dashed line) inferred from ascent rates of $\hat{H}$ anomalies and G (solid line) which is derived from the two terms above at the equator. (b) Vertical momentum advection due to the entire vertical velocity same as in top panel (dashed line), its mean component (dotted line), and its anomaly (solid line).

asymmetry of the zonal wind acceleration in Figure 8a can be generated by the QBO-induced vertical advection [*Plumb and Bell*, 1982], without considering any asymmetry in wave momentum flux divergence between the easterly and westerly acceleration [e.g., *Takahashi et al.*, 1997]. Furthermore, the easterly acceleration of G is quite larger than that in recent GCM experiments [e.g., *Takahashi et al.*, 1997], which implies more easterly momentum flux by small-scale waves and/or zonal wind tendency due to meridional wind anomalies across the equator [*Jones et al.*, 1998; *Kinnersley*, 1999]. Another candidate may be lateral propagation of planetary waves.

We further see that G is seasonally synchronized with anomalies reduced by 2–3 $\times$ 10^{-6} m s^{-2} during the Northern Hemisphere winter. This is consistent with a result that both the westerly and the easterly acceleration generally decrease during the Northern Hemisphere winter [*Dunkerton*, 1990; *Wallace et al.*, 1993]. Our result suggests that the seasonally synchronized oscillation of zonal wind acceleration can be caused by the seasonal variation of G, such as wave momentum flux [*Maruyama*, 1991] and/or meridional advection [*Jones et al.*, 1998; *Kinnersley*, 1999]. The former possibility may not be well known [e.g., *Alexander*, 1998], while global distribution of gravity wave is getting clear [*Eckermann et al.*, 1995; *Wu and Waters*, 1996; *Tsuda et al.*, 2000]. The latter effect near the easterly shear zone can be supported by the latitudinal asymmetry of easterly acceleration over the equator [*Dunkerton and Delisi*, 1985]. This implies large meridional shear of zonal wind, which may lead to large zonal wind tendency by meridional advection. On the other hand, little annual cycle of w_{tr} (Figure 3) may have small effects on the seasonal dependency of G in conflict with *Kinnersley and Pawson* [1996].

To discuss a series of possibilities, we need to examine momentum flux divergence of waves with periods shorter than a few days and meridional advection of zonal momentum in the equatorial region. At the same time, it is necessary to develop two- and three-dimensional models in which the two effects are appropriately represented.

5. Conclusions

The QBO-induced variations in vertical velocity in the lower stratosphere have been investigated with Halogen Occultation Experiment (HALOE) data from 1993 to 1998. The vertical velocity was inferred from ascent rates of an annually varying component in total water ($[H_2O] + 2[CH_4]$) at the equator.

The derived ascent rate of total water anomalies exhibits QBO variations with anomalies of 0.10–0.15 mm s^{-1} in the 20–40 hPa layer and about 0.1 mm s^{-1} near 50 hPa at the equator. In the 20–40 hPa layer the amplitude of the QBO variation may be larger than that derived from radiative calculation [*Rosenlof*, 1995; *Randel et al.*, 1999]. The QBO signal in the ascent rates showed that its negative anomalies precede positive anomalies in temperature and ozone by about 2–3 months over the equator between 30 and 60 hPa. This phase relationship is in conflict with results from two-dimensional model studies [e.g., *Jones et al.*, 1999]. The phase lag between the QBO signals in ascent rate and temperature may be explained by the observed large tendency of temperature anomalies, which is related to the rapid acceleration of the QBO westerly. It is supposed that this disagreement may be due to the observed tendency of temperature anomalies, which seems larger than that from model studies. In addition, there exists only a little annual cycle of the ascent rates around this level.

Next, the effect of momentum transport by vertical velocity in the equatorial lower stratosphere has been examined. The zonal wind acceleration by the total vertical advection calculated from the ascent rate of total water anomalies exhibits phase asymmetry between the easterly and the westerly acceleration at the equator, while the forces required to drive the observed QBO wind, which are indirectly estimated, show symmetric variations below 35 hPa. These results suggest that the well-known asymmetry of descent rates of the QBO shear regions [*Naujokat*, 1986] can be understood by the QBO-induced vertical advection and also imply a need of large easterly momentum flux as much as its westerly equivalent.

Acknowledgments. We specially wish to acknowledge fruitful discussions with Fumio Hasebe, William J. Randel, and Philip W. Mote. We are grateful to the HALOE science team for the high-quality data, and Nozomi Kawamoto for handling the HALOE data. We would like to thank Masaaki Takahashi, Noriyuki Nishi, Kaoru Sato, Holger

Vömel, Karen H. Rosenlof, Takeshi Horinouchi, Atsushi Kubokawa, and Hiroo Hayashi for discussions and comments.

References

Alexander, M. J., Interpretations of observed climatological patterns in stratospheric gravity wave variance, *J. Geophys. Res.*, *103*, 8627–8640, 1998.

Angell, J. K., and J. Korshover, Global ozone variation: An update into 1976, *Mon. Weather Rev.*, *106*, 725–737, 1978.

Canziani, P. O., and J. R. Holton, Kelvin waves and the quasi-biennial oscillation: An observational analysis, *J. Geophys. Res.*, *103*, 31,509–31,521, 1998.

Dessler, A. E., E. M. Weinstock, E. J. Hintsa, J. G. Anderson, C. R. Webster, R. D. May, J. W. Elkins, and G. S. Dutton, An examination of the total hydrogen budget of the lower stratosphere, *Geophys. Res. Lett.*, *21*, 2563–2566, 1994.

Dunkerton, T. J., On the mean meridional mass motions of the stratosphere and mesosphere, *J. Atmos. Sci.*, *35*, 2325–2333, 1978.

Dunkerton, T. J., A two-dimensional model of the quasi-biennial oscillation, *J Atmos. Sci.*, *42*, 1151–1160, 1985.

Dunkerton, T. J., Annual variation of deseasonalized mean flow acceleration in the equatorial lower stratosphere, *J. Meteorol. Soc. Jpn.*, *68*, 499–508, 1990.

Dunkerton, T. J., Nonlinear propagation of zonal winds in an atmosphere with Newtonian cooling and equatorial wave driving, *J. Atmos. Sci.*, *48*, 236–263, 1991.

Dunkerton, T. J., The role of gravity waves in the quasi-biennial oscillation, *J Geophys. Res.*, *102*, 26,053–26,076, 1997.

Dunkerton, T. J., and D. P. Delisi, Climatology of the equatorial lower stratosphere, *J. Atmos. Sci.*, *42*, 376–396, 1985.

Eckermann, S. D., I. Hirota, and W. K. Hocking, Gravity wave and equatorial wave morphology of the stratosphere derived from long-term rocket soundings, *Q J. R. Meteorol. Soc.*, *121*, 149–186, 1995.

Funk, J. P., and G. L. Garnham, Australian ozone observations and a suggested 24 month cycle, *Tellus*, *14*, 378–382, 1962.

Gray, L. J., and J. A. Pyle, A two dimensional model of the quasi-biennial oscillation of ozone, *J. Atmos. Sci.*, *46*, 203–220, 1989.

Hasebe, F., Interannual variations of global total ozone revealed from *Nimbus 4* BUV and ground-based observations, *J. Geophys Res.*, *88*, 6819–6834, 1983.

Hasebe, F., The global structure of the total ozone fluctuations observed on the time scales of two to several years, in *Dynamics of the Middle Atmosphere*, edited by J. R. Holton and T. Matsuno, pp. 445–464, Terra Sci., Tokyo, 1984.

Hasebe, F., Quasi-biennial oscillation of ozone and diabatic circulation in the equatorial stratosphere, *J Atmos. Sci.*, *51*, 1238–1242, 1994.

Haynes, P. H., C. J. Marks, M. E. McIntyre, T. G. Shepherd, and K. P. Shine, On the "downward control" of extratropical diabatic circulations by eddy-induced mean zonal forces, *J. Atmos. Sci.*, *48*, 651–678, 1991.

Holton, J. R., On the global exchange of mass between the stratosphere and troposphere, *J Atmos Sci.*, *47*, 392–395, 1990.

Holton, J. R., and R. S. Lindzen, An updated theory for the quasi-biennial cycle of the tropical stratosphere, *J. Atmos. Sci.*, *29*, 1076–1080, 1972.

Horinouchi, T., and S. Yoden, Wave-mean flow interaction associated with a QBO-like oscillation simulated in a simplified GCM, *J. Atmos. Sci.*, *55*, 502–526, 1998.

Huang, T. Y. W., The impact of solar radiation on the quasi-biennial oscillation of ozone in the tropical stratosphere, *Geophys Res Lett.*, *23*, 3211–3214, 1996.

Jackson, D. R., S. J. Driscoll, E. J. Highwood, J. E. Harries, and M. Rassell III, Troposphere to stratosphere transport at low latitudes as studies using HALOE observations of water vapour 1992–1997, *Q J R. Meteorol. Soc.*, *123*, 169–192, 1998.

Jones, D. B. A., H. R. Schneider, and M. B. McElroy, Effects of the quasi-biennial oscillation on the zonally averaged transport of tracers, *J. Geophys. Res.*, *103*, 11,235–11,249, 1998.

Jones, D. B. A., H. R. Schneider, and M. B. McElroy, An analysis of the mechanisms for the QBO in ozone in the tropical and subtropical lower stratosphere, *J. Geophys. Res.*, in press, 1999.

Jones, R. L., J. A. Pyle, J. E. Harries, A. M Zavody, J. M. Russell III, and J. C. Gille, The water vapor budget of the stratosphere studied using LIMS and SAMS satellite data, *Q. J. R. Meteorol. Soc.*, *112*, 1127–1143, 1986.

Kinnersley, J. S., Seasonal asymmetry of the low- and middle-latitude QBO circulation anomaly, *J. Atmos. Sci.*, *56*, 1140–1153, 1999.

Kinnersley, J. S., and S. Pawson, The descent rates of the shear zones of the equatorial QBO, *J. Atmos. Sci.*, *53*, 1937–1949, 1996.

Li, D., K. P. Shine, and L. J. Gray, The role of ozone-induced diabatic heating anomalies in the quasi-biennial oscillation, *Q. J. R. Meteorol. Soc.*, *121*, 937–943, 1995.

Lindzen, R. S., and J. R. Holton, A theory of the quasi-biennial oscillation, *J. Atmos. Sci.*, *25*, 1095–1107, 1968.

Ling, X.-D., and J. London, The quasi-biennial oscillation of ozone in the tropical middle stratosphere: A one-dimensional model, *J. Atmos. Sci.*, *43*, 3122–3137, 1986.

Maruyama, T., Annual variations and QBO-synchronized variations of the equatorial wave intensity in the lower stratosphere at Singapore during 1961–1989, *J. Meteorol. Soc. Jpn.*, *69*, 219–232, 1991.

Maruyama, T., Upward transport of westerly momentum due to disturbances of the equatorial lower stratosphere in the period range of about 2 days—A Singapore data analysis for 1983–1993, *J. Meteorol Soc. Jpn.*, *72*, 423–432, 1994.

Mote, P. W., K. H. Rosenlof, J. R. Holton, R. S. Harwood, and J. W. Waters, Seasonal variations of water vapor in the tropical lower stratosphere, *Geophys. Res. Lett.*, *22*, 1093–1096, 1995.

Mote, P. W., K. H. Rosenlof, M. E. McIntyre, E. S. Carr, J. C. Gille, J. R. Holton, J. S. Kinnersley, H. C. Pumphrey, J. M. Russell III, and J. W. Waters, An atmospheric tape recorder: The imprint of tropical tropopause temperatures on stratospheric water vapor, *J. Geophys. Res.*, *101*, 3989–4006, 1996.

Mote, P. W., T. J. Dunkerton, M. E. McIntyre, E. A. Ray, and P. H. Haynes, Vertical velocity, vertical diffusion, and dilution by midlatitude air in the tropical lower stratosphere, *J. Geophys. Res.*, *103*, 8651–8666, 1998.

Murgatroyd, R. J., and F. Singleton, Possible meridional circulations in the stratosphere and mesosphere, *Q. J. R. Meteorol. Soc.*, *87*, 125–135, 1961.

Naujokat, B., An update of the observed quasi-biennial oscillation of the stratospheric winds over the tropics, *J. Atmos. Sci.*, *43*, 1873–1877, 1986.

Olaguer, E. P., H. Yang, and K. K Tung, A re-examination of the radiative balance of the stratosphere, *J Atmos. Sci.*, *49*, 1242–1263, 1992.

Oltmans, S. J., and J. London, The quasi-biennial oscillation in atmospheric ozone, *J. Geophys. Res.*, *87*, 8981–8989, 1982.

Plumb, R. A., and R. C. Bell, A model of the quasi-biennial oscillation on an equatorial beta-plane, *Q. J. R. Meteorol. Soc.*, *108*, 335–352, 1982.

Plumb, R. A., and J. Eluszkiewicz, The Brewer-Dobson circulation: Dynamics of the tropical upwelling, *J. Atmos. Sci.*, *56*, 868–890, 1999.

Ramanathan, K. R., Bi-annual variation of atmospheric ozone over the tropics, *Q. J. R. Meteorol. Soc.*, *89*, 540–542, 1963.

Randel, W. J., and A. Cobb, Coherent variations of monthly mean total ozone and lower stratospheric temperature, *J Geophys. Res.*, *99*, 5433–5447, 1994.

Randel, W. J., and F. Wu, Isolation of the ozone QBO in SAGE II data by singular value decomposition, *J. Atmos. Sci.*, *53*, 2546–2559, 1996.

Randel, W. J., F. Wu, J. M. Russell III, and A. Roche, Seasonal cycles and QBO variations in stratospheric CH_4 and H_2O observed in UARS HALOE data, *J. Atmos. Sci.*, *55*, 163–185, 1998.

Randel, W. J., F. Wu, R. Swinbank, J. Nash, and A. O'Neil, Global QBO circulation derived from UKMO stratospheric analyses, *J. Atmos. Sci.*, *56*, 457–474, 1999.

Reed, R. J., A tentative model of the 26-month oscillation in tropical latitudes, *Q. J. R. Meteorol. Soc.*, *90*, 441–466, 1964.

Reed, R. J., W. J. Campbell, L. A. Rasmussen, and D. G. Rogers, Evidence of downward propagating annual wind reversal in the equatorial stratosphere, *J. Geophys. Res.*, *66*, 813–818, 1961.

Remsberg, E. E., P. P. Bhatt, and J. M. Russell III, Estimates of the water vapor budget of the stratosphere from UARS HALOE data, *J. Geophys. Res.*, *101*, 6749–6766, 1996.

Rosenlof, K. H., Seasonal cycle of the residual mean circulation in the stratosphere, *J. Geophys. Res.*, *100*, 5173–5191, 1995.

Rosenlof, K. H., and J. R. Holton, Estimates of the stratospheric residual circulation using the downward control principle, *J. Geophys. Res.*, *98*, 10,465–10,479, 1993.

Russell, J. M. III, L. L Gordley, J. H. Park, S. R. Drayson, W. D. Haskett, R. J. Cicerone, A. F. Tuck, J. E. Frederick, J. E. Harries,

and P. J. Crutzen, The Halogen Occultation Experiment, *J. Geophys. Res.*, *98*, 10,777–10,797, 1993.

Sato, K., and T. J. Dunkerton, Estimates of momentum flux associated with equatorial Kelvin and gravity waves, *J. Geophys. Res.*, *102*, 26,247–26,261, 1997.

Sato, K., F. Hasegawa, and I. Hirota, Short-period disturbances in the equatorial lower stratosphere, *J. Meteorol. Soc. Jpn.*, *72*, 859–872, 1994.

Shiotani, M., Annual, quasi-biennial, and El Ninō-Southern Oscillation (ENSO) timescale variations in equatorial total ozone, *J. Geophys. Res.*, *97*, 7625–7633, 1992.

Shiotani, M., and F. Hasebe, Stratospheric ozone variations in the equatorial region as seen in SAGE data, *J. Geophys. Res.*, *99*, 14,575–14,584, 1994.

Takahashi, M., N. Zhao, and T. Kumakura, Equatorial waves in a general circulation model simulating a quasi-biennial oscillation, *J. Meteorol. Soc. Jpn.*, *75*, 529–540, 1997.

Tsuda, T., and M. Nishida, A global morphology of gravity wave activity in the stratosphere reveraled by the GPS occultation data, *J. Geophys. Res.*, *105*, 7257–7273, 2000.

Veryard, R. G., and R. A. Ebdon, Fluctuations in tropical stratospheric winds, *Meteorol. Mag.*, *90*, 125–143, 1961.

Wallace, J. M., L. Panetta, and J. Estberg, A phase-space representation of the equatorial stratospheric quasi-biennial oscillation, *J. Atmos. Sci.*, *50*, 1751–1762, 1993.

Wu, D. L., and J. Waters, Satellite observations of atmospheric variances: A possible indication of gravity waves, *Geophys. Res. Lett.*, *23*, 3631–3634, 1996.

Zawodny, J. M., and M. P. McCormick, Stratospheric Aerosol and Gas Experiment II measurements of the quasi-biennial oscillation in ozone and nitrogen dioxide, *J. Geophys. Res.*, *96*, 9371–9377, 1991.

M. Niwano and M. Shiotani, Division of Ocean and Atmospheric Sciences, Graduate School of Environmental Earth Science, Hokkaido University, 10 Kita, 5 Nishi, Sapporo 060-0810, Japan. (niwano@ees.hokudai.ac.jp)

(Received February 23, 2000; revised September 7, 2000;
accepted October 24, 2000.)